ECMWF soil moisture data assimilation

Janneke Ettema and Pedro Viterbo

ECMWF, Shinfield Park, Reading
RG2 9AX, United Kingdom
J.Ettema@ECMWF.int, P.Viterbo@ECMWF.int

1. Introduction

Soil moisture is a crucial variable for numerical weather prediction (NWP) models, because it acts as a lower boundary condition. It strongly influences the partitioning of available energy into sensible and latent heat flux and hence the evolution of the lower atmospheric conditions. Imperfect parameterisations of land surface and soil processes and failures in simulating precipitation and cloud cover can lead to considerable drifts of soil moisture; assimilation is needed to control forecast drifts. The use of in-situ observations is unfeasible, because no extensive observation network exists. A number of studies explore the use of different observation types with various assimilation methods. Conventional data, e.g. screen-level parameters (T_{2m} and RH_{2m}), and satellite data, e.g. surface radiative temperature and passive microwave brightness temperatures (SRT and T_B), can be used to adjust soil moisture in an assimilation framework.

Within the ELDAS project (European Land Data Assimilation System) the performance of the Optimal Interpolation (OI) method and a simplified extended Kalman filter (EKF) for soil moisture analysis on T_{2m} and RH_{2m} are compared. The EKF method is flexible to accommodate new observation types using a 24-h assimilation window. To investigate if the assimilation of different observation types improves the simulated soil moisture, model runs with different combinations of T_{2m}, RH_{2m}, L-band T_B and measured skin temperature are compared with independent observations. Both assimilation systems are tested with the single-column version (SCM) of the ECMWF model. Three hourly observations of precipitation based on high-density gauges, and incoming shortwave and longwave radiation based on METEOSAT data were used as forcing parameters, replacing model values every time step.

The following Section will describe the ELDAS data assimilation system, the single-column test-bed, and the observation experiments. Section 3 compares OI and EKF, present examples of synergy of observations and the impact of forecast data, while in Section 4 conclusions and perspectives are presented. Additional details about the tested data assimilation systems and set-up of the SCM-experiments described here can be found in Sueffert et al. (2003, 2004).

2. The ELDAS data assimilation system at ECMWF

2.1. The simplified Extended Kalman Filter analysis

Within the framework of the ELDAS project a new soil moisture analysis system was developed using a simplified extended Kalman filter (EKF) based on Hess (2001). The simulated soil moisture in the three soil layers is improved by minimizing the classical cost function $\boldsymbol{J}$ by optimally combining the information from the model forecast (or background) of state vector $\mathbf{x}_b$ and observed parameters, specified in the observation vector $\mathbf{y}$:

$$\boldsymbol{J}(\mathbf{x}) = (\mathbf{x}-\mathbf{x}_b)^T \mathbf{B}^{-1}(\mathbf{x}-\mathbf{x}_b) + [\boldsymbol{y}-\boldsymbol{H}(\mathbf{x})]^T \mathbf{R}^{-1}[\boldsymbol{y}-\boldsymbol{H}(\mathbf{x})] \tag{1}$$

where $\boldsymbol{H}$ denotes the observation operator, $\mathbf{B}$ and $\mathbf{R}$ denote the background and observation error covariances, respectively. The assumption is made that for quasi-linear problems the minimum of $\boldsymbol{J}$ can be directly derived rather than applying an iterative method (Hess 2001). The analysis increment is at time $\boldsymbol{i}$:

$$\mathbf{x}_{\boldsymbol{a}}(\boldsymbol{i})-\mathbf{x}_{\boldsymbol{b}}(\boldsymbol{i})=\mathbf{K}_{[\boldsymbol{i},\boldsymbol{i}+\mathbf{24}]}(\boldsymbol{y}_{[\boldsymbol{i},\boldsymbol{i}+\mathbf{24}]}-\mathbf{H}_{[\boldsymbol{i},\boldsymbol{i}+\mathbf{24}]}\mathbf{x}_{\boldsymbol{b},[\boldsymbol{i},\boldsymbol{i}+\mathbf{24}]}) \tag{2}$$

where $\mathbf{H}$ is the linearized $\boldsymbol{H}$ and $\mathbf{K}$ the gain matrix expressed in model space:

$$\mathbf{K}_{[\boldsymbol{i},\boldsymbol{i}+\mathbf{24}]}=[\mathbf{B}^{-1}(\boldsymbol{i})+\mathbf{H}^{\boldsymbol{T}}_{[\boldsymbol{i},\boldsymbol{i}+\mathbf{24}]}\mathbf{R}^{-1}\mathbf{H}_{[\boldsymbol{i},\boldsymbol{i}+\mathbf{24}]}(\boldsymbol{i})]^{-1}\mathbf{H}^{\boldsymbol{T}}_{[\boldsymbol{i},\boldsymbol{i}+\mathbf{24}]} \tag{3}$$

where $[\boldsymbol{i},\boldsymbol{i}+24]$ indicates the 24-h window. The tangent linear of the observation operator is approximated by a one side finite difference assuming that close to the background state, the state parameters depend linearly on the observation variables. Therefore, for each state variable one additional forecast run with initial perturbations is required. This way no adjoint or tangent linear model is needed. The background error covariance evolves temporally with a 24-h cycling according to:

$$\mathbf{B}(\boldsymbol{i}+\mathbf{24})=\mathbf{M}_{\boldsymbol{i}\to\boldsymbol{i}+\mathbf{24}}\mathbf{A}(\boldsymbol{i})\mathbf{M}^{\boldsymbol{T}}_{\boldsymbol{i}\to\boldsymbol{i}+\mathbf{24}}+\mathbf{Q}(\boldsymbol{i}) \tag{4}$$

where $\mathbf{Q}$ is the model error covariance matrix and $\mathbf{M}$ is the full non-linear model. The model error covariance matrix is assumed to be diagonal and constant in time. The standard deviations for the observation errors are set to 2K for T_{2m}, 10% for RH_{2m} and 2K for T_B. We assume that the observation and model errors are mutually uncorrelated and white. The updated analysis error matrix, $\mathbf{A}$, is calculated by:

$$\mathbf{A}(\boldsymbol{i})=[\mathbf{B}^{-1}(\boldsymbol{i})+\mathbf{H}^{\boldsymbol{T}}_{[\boldsymbol{i},\boldsymbol{i}+\mathbf{24}]}\mathbf{R}^{-1}\mathbf{H}_{[\boldsymbol{i},\boldsymbol{i}+\mathbf{24}]}(\boldsymbol{i})]^{-1} \tag{5}$$

In contrast to the original algorithm, described by Hess (2001), we account for the soil water transfer between the layers in the calculation of the forecast error covariance. The start values for the following day $(\boldsymbol{i}+24\text{h})$ are calculated by:

The advantage of this soil moisture analysis scheme is that forecast errors depend on the synoptic situation and are not fixed to statistically derived values as in a optimal interpolation system. More details can be found in Sueffert et al. (2004).

2.2. The single column system

The soil moisture analysis systems are tested with the Single Column Model (SCM) of the ECMWF NWP model (cycle version 23R4). The SCM is a hydrostatic model based on the primitive equations incorporating 60 atmospheric levels with a well-resolved boundary layer. It includes the comprehensive physical package as used in the operational NWP model. The SCM incorporates a land surface model TESSEL (Tiled ECMWF Scheme for Surface Exchanges over Land; Viterbo and Beljaars 1995; van den Hurk et al. 2000). TESSEL employs four soil layers (0.07, 0.21, 0.72, and 1.68 m) where the top three layers cover most of the root zone for all vegetation types. The vertical water transport follows Darcy’s law and free drainage at the bottom. Soil heat budget is calculated based on Fourier diffusion law. For six different land tiles the surface energy balance is solved separately with regard to the skin temperature. Sensible and latent heat flux for each tile are parameterised by resistance-based formulations. The leaf area index (LAI) is a function of vegetation type, with no seasonality. The same soil type is specified globally.

All model runs start at local midnight and are initialised every 24 hours with atmospheric ERA40 re-analysis data. Soil moisture and soil temperatures evolve freely (in control simulations) or are modified by data assimilation. Precipitation and incoming shortwave and longwave radiation are prescribed every 20 minutes (equals model time step) from observations to avoid errors in the main forcing to the land surface scheme.

To simulate L-band T_B the SCM is coupled to a LSMEM (Land Surface Microwave Emissivity Model; Drusch et al., 2001). The LSMEM takes vegetation, rough surface and atmospheric contributions into account dealing with frequencies between 1.4-20 GHz.

2.3. Description of the experiments

2.3.1. FIFE87

The two assimilation schemes are compared for data from the First International Satellite Land Surface Climatology Project (SLSCP) Field Experiment (FIFE) (Betts and Ball 1998). Observations are made on a 15x15 km site in the Konza prairie, Kansas. The dataset for the period 1 June-9 October 1987 consists of near-surface atmospheric parameters, radiative forcing, soil moisture, temperature and heat fluxes observations. Both soil moisture analysis systems incorporate observations of screen-level parameters.

2.3.2. SGP97

To test the synergy of the different observation types, data from the SGP97 experiment (Southern Great Plains for the period 18 June-17 July 1997; Betts and Ball 1998) were used. For three investigation areas L-band observations from aircraft is combined with ground measurements. This study focuses on the Little Washita River watershed observation site (LW02). On this site a long-term flux monitoring site was operated that provide measurements of near-surface atmospheric and soil parameters. Observations of 1.4-GHz brightness temperature were provided by the Electronically Scanned Thinned Array Radiometer (ESTAR; Le Vine et al. 1994), which was mounted on an aircraft.

2.3.3. MUREX97

To investigate the assimilation of rate of change of surface radiative temperature data were used from the MUREX experiment (Monitoring the Usable Soil Reservoir Experimentally; Calvet and Noilhan 2000). For the period June 1994 to May 1999 a meteorological station was operated on a fallow land in Southern France. The surface radiative temperature was derived from infrared radiometry. In this study data from 1 June-9 October 1997 are used.

2.3.4. ELDAS validation points

To evaluate the impact of precipitation and incoming radiation forcing, one of the ELDAS validation points is chosen, Loobos, the Netherlands. Three hourly precipitation of precipitation are based on high-density network of rain-gauges (Rubel 2004) and incoming shortwave and longwave radiation are based on METEOSAT data (Meetschen et al. 2004). All simulations and datasets span a 15-month period (October 1999 up to December 2000).

3. Results

3.1. Optimal Interpolation versus Extended Kalman Filter

The main differences between the OI and EKF data assimilation systems concern the calculations of the forecast errors. Compared to the OI method the forecast errors of EKF system depend on the weather regime, rather than being fixed to statistically derived values. The temporal evolution of the gain matrix $\mathbf{K}$ can be represented by the Froebenius norm (FN):

$$\|\mathrm{FN}\| = \sqrt{\sum_{\boldsymbol{l}=1}^{3} \sum_{\boldsymbol{m}=1}^{6} \left(\boldsymbol{k}_{\boldsymbol{lm}}^{2}\right)} \tag{6}$$

with $\boldsymbol{l}$ and $\boldsymbol{m}$ indexing the number of soil layers and observations, respectively. In Figure 1 the Froebenius norm of the OI and EKF systems are plotted for FIFE site (Betts and Ball 1998).

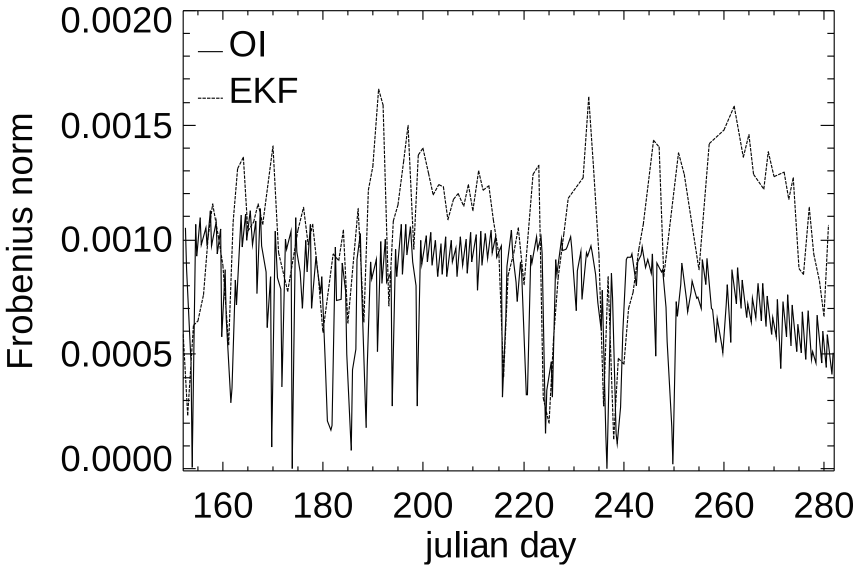

Figure 1: Evolution of the Froebenius norm of the gain matrix for the OI and EKF analysis system (1 Jun - 9 Oct 1987 for FIFE).

In general, the FN of OI and EKF evolve similarly (Figure 1). Both systems distinguish between periods of strong and weak influence screen-level parameters on soil moisture. The OI system adjusts to the atmospheric situations due to atmospheric criteria whereas EKF has its built-in dynamic dependency due to the built-in dynamical dependency. In clear-sky conditions, the FN of the EKF system is slightly larger than FN of OI, which means that the EKF method has a slight preference for the observations rather than the background.

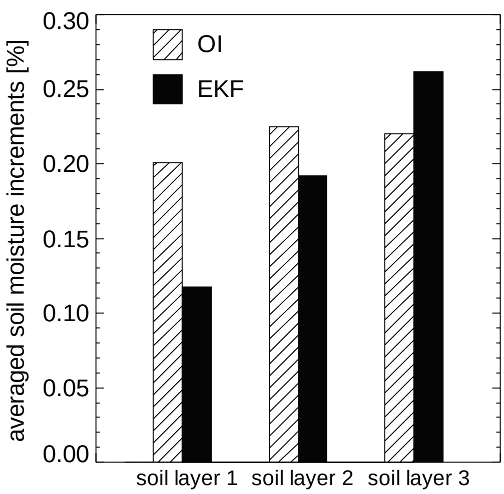

Figure 2: Comparison of the averaged soil moisture increments over 130 days (FIFE87) for each soil layer derived by OI and EKF analysis system.

The soil moisture increments of the EKF system are of the same order as those of OI (Figure 2). The OI increments are similar across the three top layers, whereas the EKF system puts more weight on the deeper layers. This is a result of taking the water transport between the soil layers into account when updating forecast errors.

3.2. Synergy of observation types

To test and compare the performance of assimilating a combination of screen-level parameters and remotely sensed observations only the EKF system is applied with using the SGP97 dataset. The following model runs are conducted: the first one is a control run without soil moisture analysis, but with free running soil moisture and soil temperature (CTRL). In KTR-runs T_{2m} and RH_{2m} are assimilated and in KB-runs L-band T_B is assimilated. In the fourth run, KTRB, all three types of observations are assimilated.

Figure 3a, b and 4 show the temporal evolution of the assimilated parameters T2m, RH2m and TB for the four simulations in comparison with the observations. All four simulations underestimate daily mean RH2m and overestimate daily mean T2m. As expected, assimilation of screen-level parameters decreases the warm and dry bias considerably in the KTR- and KTRB-runs. In general, the best fit to the observed screen-level parameters is achieved when all three parameters are assimilated, because problems with one observation type, e.g. missing data, are compensated by another data type, or the signals intensify each other.

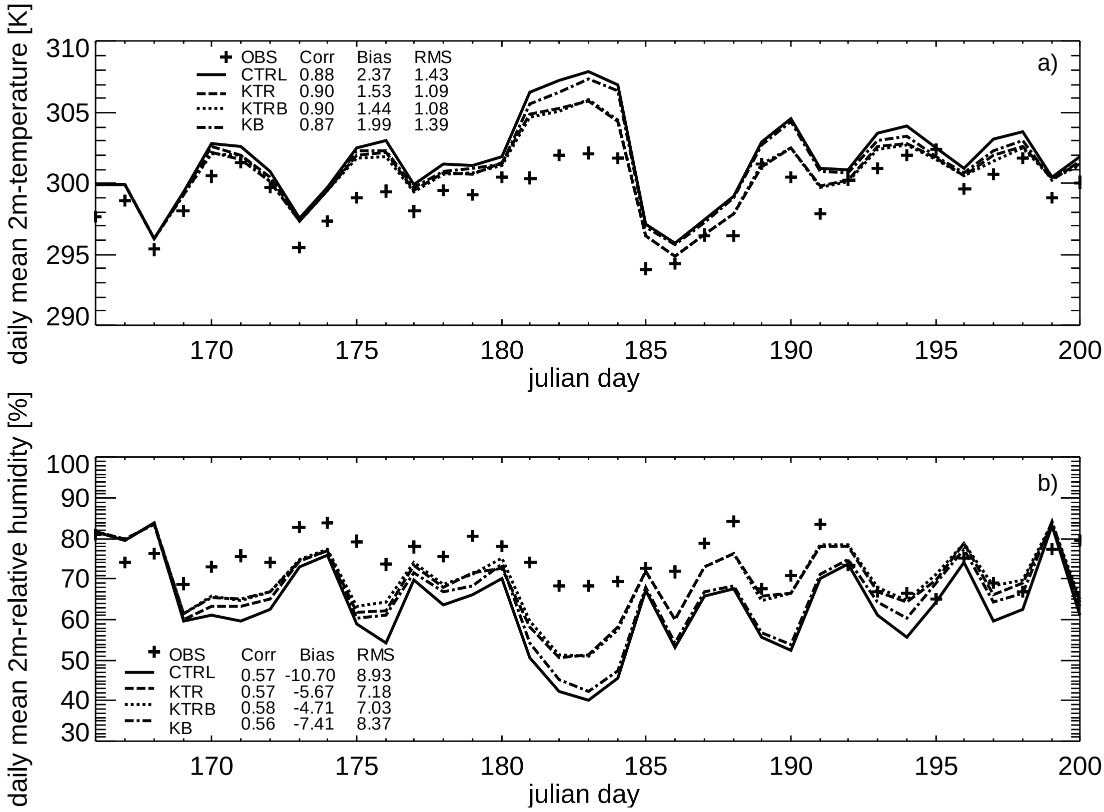

Figure 3: Temporal evolution for 15 June - 19 July 1997 of a) 2-m temperature and b) 2-m relative humidity simulated by the CTRL-, KTR-, KTRB-,and KB-runs in comparison to observations from SGP97.

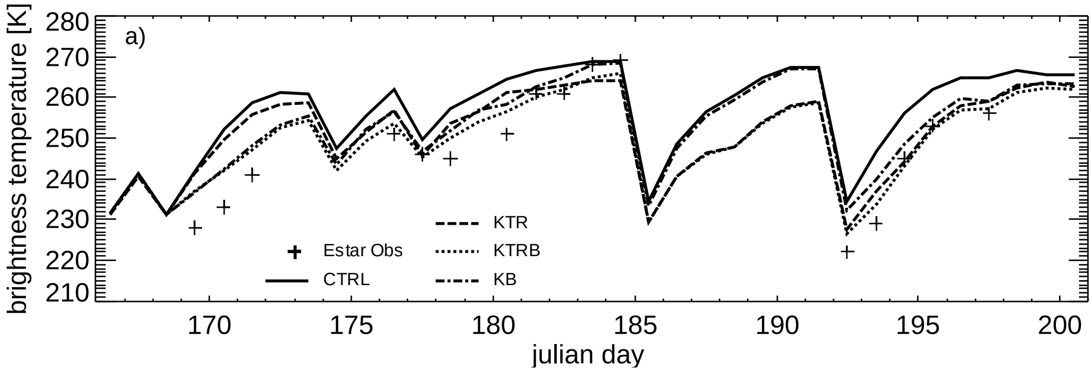

Figure 4: The same as in Figure 3 except for 1.4-GHz microwave brightness temperature.

In general, all four model runs overestimate observed TB (Figure 4) because of an underestimation of the surface soil moisture (not shown). The assimilation of screen-level parameters already slightly reduced simulated TB. The use of TB improves the simulations clearly, but the observed brightness temperature is captured best when T2m, RH2m, and TB are assimilated.The root zone soil moisture is best captured by the CTRL- and the KB-run (Figure 5). In the KTR- and KTRB-runs water is added to the soil though no precipitation was observed. This means that soil moisture is used to compensate for non-soil-moisture-related deficiencies in the experiment setup. These deficiencies could be a misrepresentation of land surface processes or atmospheric processes (e.g. advection) that causes a colder and moister atmosphere and not due to a higher root zone soil water content.

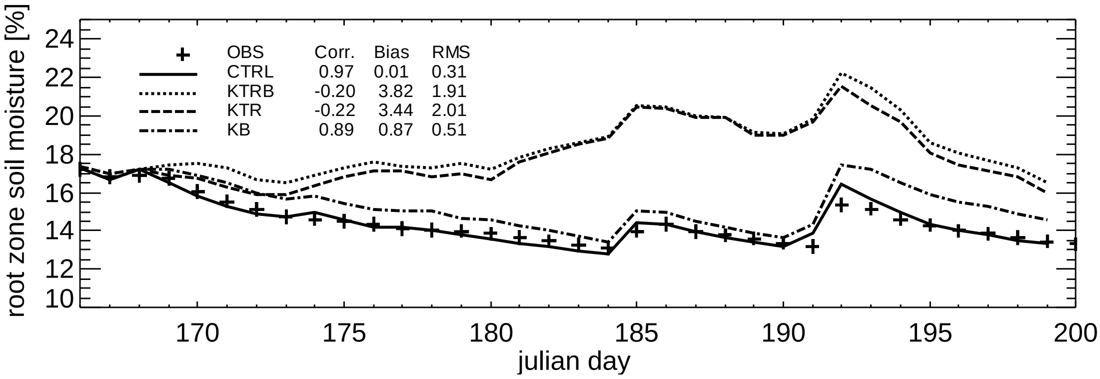

Figure 5: The same as Figure 3 except for the root zone moisture.

In most NWP models evaporative fraction, defined as EF=LE/(LE+H), is the relevant quantity for the surface impact on the atmosphere. In Figure 6 the observed evaporative fraction shows only slight day-to-day variation, while the simulation of the CTRL-run varies substantially. The assimilation of T_B on its own is not effective enough to change evaporative fraction. The day-to-day variation is clearly reduced when screen-level parameters are used. The best results are achieved with the synergy of screen-level parameters and T_B, because the different observation types complement each other.

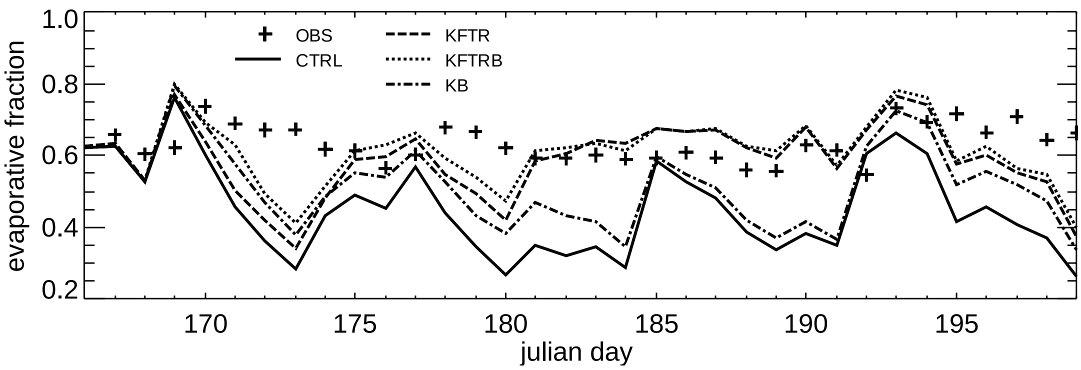

Figure 6: The same as Figure 3 except for evaporative fraction.

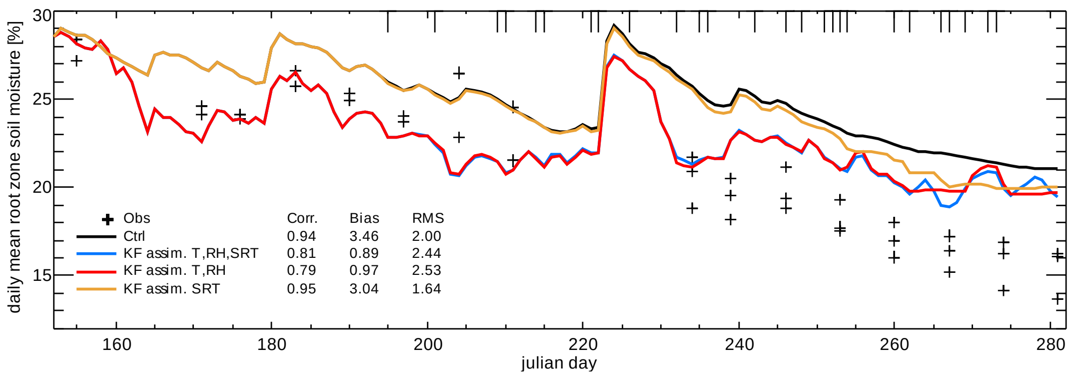

Figure 7: Temporal evolution for 1 Jun - 9 Oct 1997 of root zone moisture simulated by the CTRL-, and EKF-runs assimilating T, RH, w/ or w/o SRT in comparison to observations.

For MUREX97 experiment surface radiative temperatures (SRT) are measured, of which the early morning evolution is linked to evaporation and includes information about the root zone soil moisture. To evaluate its additional information on soil moisture these observations are included in assimilation simulations and compared to the assimilation of screen-level parameters.

In Figure 7 the spikes at the top indicate the days observations are available (50% of the data was missing and 25% during cloudy situations). The assimilation of rate of change of surface radiative temperature gives little extra information about the mean root zone soil moisture when screen-level parameters are present. Low data coverage during this experiment does not allow for real conclusion.

3.3. Impact of forcing data

For testing the soil moisture analysis systems with different observation types precipitation and incoming radiation data were prescribed by observations. To study the influence of replacing surface forcing with observed values, four configurations all without soil moisture data assimilation are compared: a) a run with both observed forcings (CTRL), b) a run with no observed forcings (NO FORC), c) a run with no observed precipitation, only radiation (NO PREC), and d) a run with no observed radiation, only precipitation (NO RAD).

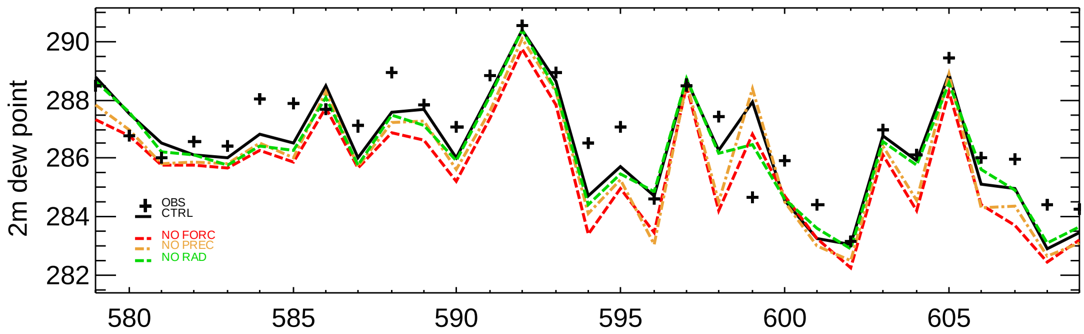

Figure 8: Temporal evolution for August 2000 of daily mean value of 2-m dew point temperature simulated by the CTRL-, no forc-, no prec-, and no rad-runs in comparison to observations.

Figure 8 shows the effect of the forcing data on the daily values of 2-metre dew point temperature for Loobos, the Netherlands. The positive impact of the observations, especially precipitation, is clear; when especially precipitation observations are omitted the model drifts dry. This means that correct forcing of precipitation and incoming radiation is essential to get the conditions at the surface correct.

4. Conclusions

The single column model test bed proved to be an invaluable tool to develop, test and validate data assimilation systems. To improve the soil moisture initial conditions for numerical weather prediction models two different soil moisture analysis systems based on both screen-level parameters and 1.4 GHz brightness temperature are investigated. The performance of a simplified Extended Kalman Filter system and an Optimal Interpolation method assimilating screen-level parameters are explored. Both systems show similar temporal evolution of the gain matrix and size of the soil moisture increments. The EKF method is more flexible to accommodate for several types of observations using a 24-h assimilation window.

To investigate whether the assimilation of different observation types improves the simulation, model runs with different combinations of T_{2m}, RH_{2m}, L-band T_B and measured skin temperature are compared with independent observations for SGP97 and MUREX97. In general the synergy of observations related to evaporation (T_{2m}, RH_{2m}, and clear-sky radiances) together with those linked to top soil moisture (L-band radiometry) provides complementary information and reduces the risks of aliasing. To improve the screen-level forecasts and root zone soil moisture appears to be difficult to achieve at the moment. NWP models tend to tune the assimilation to fit the evaporative fraction since that is the quantity impacting on the atmosphere. Before the inclusion of new observation types for land-surface analyses model improvements are needed. Evaluation of the surface forcing data shows that precipitation input into land surface models remains one of the main sources of uncertainty.

Work will start soon to use a version of the ELDAS EKF system in operations. The system will be able to include new observation types, for example, the forthcoming L-band data from SMOS and HYDROS and, probably, existing active and passive C-band data from scatterometers and AMSR-E, respectively. The inclusion of these new observational types for land surface analysis will expose deficiencies in the background model suggesting directions for new improvements regarding soil types and soil hydrology. Therefore, the inclusion of new observations in soil moisture data assimilation will improve the quality of the analysed soil moisture, but in the long term it increases the realism of the land surface model.

References

Betts, A. K. and J. H. Ball (1998). FIFE surface climate and site-averaged dataset 1987-1989. *J. Atmos. Sci. 55,* 352-470.

Calvet, J.-C. and J. Noilhan (2000). From near-surface to root-zone soil moisture using year-round data. *J. Hydrometeorol. 1,* 393-411.

Douville, H., P. Viterbo, J.-F. Mahfouf, and A. C. M. Beljaars (2000). Evaluation of the optimum interpolation and nudging techniques for soil moisture analysis using FIFE data. *Mon. Wea. Rev. 128,* 1733-1756.

Drusch, M., E.F. Wood, and T.J. Jackson (2001). Vegetative and atmospheric corrections for the soil moisture retrieval from passive microwave remote sensing data: Results from the Southern Great Plains hydrology Experiment 1997. *J. Hydrometeorol. 2,* 181-192.

Hess, H. (2001). Assimilation of screen-level parameters by variational soil moisture analysis. *Meteorol. Atmos. Phys. 77,* 145-154.

Le Vine, D. M., A. J. Griffis, C. T. Swift, and T.J. Jackson (1994).ESTAR: A synthetic aperture microwave radiometer for remote sensing applications. *Proc. IEEE. 82,* 1787-1801.

Meetschen, D., B.J.J.M. van den Hurk, F. Ament, and M. Drusch (2004): Optimized surface radiation fields derived from METEOSAT imagery and a regional atmospheric model, *J. Hydrometeorol. 5,1091-1101*

Rubel, F. (2004): A New European Precipitation Dataset for NWP Model Verification and Data Assimilation Studies, Research Activities in Atmospheric and Oceanic Modelling, Edition 2004, Section 2, 15-16, WMO/TD available at http://www.cmc.ec.gc.ca/rpn/wgne/

Sueffert, G., H. Wilker, P. Viterbo, M. Drusch, and J.-F. Mahfouf (2004). The usage of screen-level parameters and microwave brightness temperature for soil moisture analysis. *J. Hydrometeor. 5,* 516-531.

Sueffert, G, H. Wilker, P. Viterbo, J.-F. Mahfouf, M. Drusch, and J.-C. Calvet (2003). Soil moisture analysis combining screen-level parameters and microwave brightness temperature: a test with field data. *Geophys. Res. Lett. 30,* 1498.

Van den Hurk, B. J. J., P. Viterbo, A. C. M. Beljaars, and A. K. Betts (2000). Offline validation of the ERA40 surface scheme. *ECMWF Tech. Mem. 295,* 42 pp.

Viterbo, P. and A. C. M. Beljaars (1995). An improved land surface parameterisation scheme in the ECMWF model and its validation. *J. Climate 8,* 2716-2748.